Published in final edited form as:
Clin Oral Implants Res. 2011 August ; 22(8): 865–872. doi:10.1111/j.1600-0501.2010.02074.x.

Osteoblast response to titanium surfaces functionalized with extracellular matrix peptide biomimetics

B. F. Bell
Institute for Bioengineering and Bioscience, Georgia Institute of Technology, Atlanta, GA, USA

M. Schuler
Laboratory for Surface Science and Technology, Department of Materials, ETH Zurich, Zurich, Switzerland

Institut Straumann AG, Basel, Switzerland

S. Tosatti and **M. Textor**
Laboratory for Surface Science and Technology, Department of Materials, ETH Zurich, Zurich, Switzerland

Z. Schwartz and **B. D. Boyan**
Institute for Bioengineering and Bioscience, Georgia Institute of Technology, Atlanta, GA, USA

Abstract

Objective—Functionalizing surfaces with specific peptides may aid osteointegration of orthopedic implants by favoring attachment of osteoprogenitor cells and promoting osteoblastic differentiation. This study addressed the hypothesis that implant surfaces functionalized with peptides targeting multiple ligands will enhance osteoblast attachment and/or differentiation. To test this hypothesis, we used titanium (Ti) surfaces coated with poly-L-lysine-grafted polyethylene glycol (PLL-*g*-PEG) and functionalized with two peptides found in extracellular matrix proteins, arginine–glycine–aspartic acid (RGD) and lysine–arginine–serine–arginine (KRSR), which have been shown to increase osteoblast attachment. KSSR, which does not promote osteoblast attachment, was used as a control.

Materials and methods—Sandblasted acid-etched titanium surfaces were coated with PLL-*g*-PEG functionalized with varying combinations of RGD and KRSR, as well as KSSR. Effects of these surfaces on osteoblasts were assessed by measuring cell number, alkaline phosphatase-specific activity, and levels of osteocalcin, transforming growth factor beta-1 (TGF-β1), and PGE_2.

Results—RGD increased cell number, but decreased markers for osteoblast differentiation. KRSR alone had no effect on cell number, but decreased levels of TGF-β1 and PGE_2. KRSR and RGD/KRSR coatings inhibited osteoblast differentiation vs. PLL-*g*-PEG. KSSR decreased cell number and increased osteoblast differentiation, indicated by increased levels of osteocalcin and PGE_2.

Corresponding author:*Barbara D. Boyan*, Department of Biomedical Engineering, Georgia Institute of Technology, 315 Ferst Drive NW Atlanta, GA 30332-0363, USA, Tel.: +404 385 4108, Fax: +404 894 2291, barbara.boyan@bme.gatech.edu.

Conclusions—The RGD and KRSR functionalized surfaces supported attachment but did not enhance osteoblast differentiation, whereas KSSR increased differentiation. RGD decreased this effect, suggesting that multifunctional peptide surfaces can be designed that improve peri-implant healing by optimizing attachment and proliferation as well as differentiation of osteoblasts, but peptide combination, dose and presentation are critical variables.

Keywords

KRSR; KSSR; microstructure; non-fouling; osteoblast differentiation; PLL-*g*-PEG; RGD; surface modification; surface roughness; titanium

Dental implant surfaces have been functionalized with specific proteins or peptides to aid osteointegration by favoring attachment of bone-forming osteoblasts or osteoprogenitor cells and promoting osteoblastic differentiation and the formation of mineralized bone matrix (Garcia & Reyes 2005; Morra 2006; Schuler et al. 2006a, 2006b). Surfaces that have rough microtopographies enhance osteoblast differentiation *in vitro* and increase implant pull-out strength *in vivo* (Boyan et al. 2001; Schwartz et al. 2008). When these substrates are functionalized with peptides known to enhance osteoblast attachment such as RGD, the stimulatory effect of microstructure on osteoblast differentiation is reduced (Tosatti et al. 2004). Recent studies indicate that the combination of osteoblast-specific ligands with rough surface microtopographies could potentially increase early osteoblast attachment and differentiation to better promote osteointegration and improve long-term implant fixation (Schuler et al. 2006a, 2006b). The purpose of the present study was to test this hypothesis by examining the response of osteoblasts to microstructured Ti substrates functionalized with RGD together with a biomimetic peptide KRSR, shown previously to selectively increase osteoblast attachment to tissue culture polystyrene (TCPS) and KSSR, which lacks this functionality (Dee et al. 1998).

The RGD motif is found in various extracellular matrix proteins, including fibronectin, vitronectin, osteopontin, and bone sialoprotein (Pierschbacher & Ruoslahti 1984; Ruoslahti & Pierschbacher 1987; Ruoslahti 1996). Depending on howitispresented in itsnativeprotein, it is recognized by multiple integrins including $\alpha_v\beta_3$. RGD isalsorecognizedby the $\alpha_5\beta_I$ integrin, an integrin that is highly expressed in osteoblasts, although high-affinity binding of $\alpha_5\beta_I$ to RGD requires the PHSRN synergy site to maximize the activation of osteoblastic signaling pathways (Cutler & Garcia 2003). By itself, RGD has been shown to increase cell attachment and proliferation (Ruoslahti & Pierschbacher 1987; Ruoslahti 1996), including the attachment and proliferation of osteoblasts to TCPS (Dee et al. 1998; Schuler et al. 2006a, 2006b). When immature osteoblasts were grown on SLA that were coated with PLL-*g*-PEG functionalized with a linear RGD peptide, the RGD peptide blocked the stimulatory effect of the PLL-*g*-PEG coating on differentiation but it did not modify the response of the cells to the microstructure of the Ti substrate (Tosatti et al. 2004). These studies suggested that osteoblast differentiation was promoted by substrates that fostered reduced spreading like microstructured Ti (Boyan et al. 2001) and PLL-*g*-PEG (Tosatti et al. 2004).

In vivo, RGD has been reported to increase osteointegration in some studies (Elmengaard et al. 2005; Germanier et al. 2006; Schuler et al. 2006a, 2006b), but not others (Barber et al.

2007; Petrie et al. 2008). The biological activity of RGD is less potent than that of native fibronectin or the fibronectin fragment FNIII7-10 (Garcia & Reyes 2005; Petrie et al. 2006). This suggests that the linear RGD peptide alone may be insufficient for optimal interaction of the cell with its substrate or extracellular matrix. Alternatively, a combination of binding domains presented in the proper spatial configuration may be necessary to maximize biological activity (Healy et al. 1999; Dettin et al. 2002; Reyes & Garcia 2004; Garcia 2005; Cavalcanti-Adam et al. 2006, 2007). The present study was based on the hypothesis that osteoblast attachment, proliferation, and differentiation on a microstructured-Ti surface could be enhanced by a biomimetic pep-tide coating that presented a combination of amino acid motifs that targeted two different signaling pathways: RGD to target integrin signaling and KRSR to target transmembrane proteoglycans. KRSR was designed based on its basic–basic–nonbasic–basic (BBXB) amino acid charge structure that was proposed by Cardin & Weintraub (1989) to bind heparan sulfate, a component of transmembrane proteoglycans expressed by osteoblasts. BBXB patterns are also found in various bone adhesive proteins including fibronectin, vitronectin, bone sialoprotein, thrombospondin, and osteopontin (Dee et al. 1998). KRSR was shown to selectively increase osteoblast attachment to TCPS relative to uncoated controls (Dee et al. 1998). In contrast, KSSR, which has a basic–nonbasic–nonbasic– basic (BXXB) amino acid charge structure, did not support attachment. These two peptides differ in only one amino acid residue, demonstrating the specificity of the KRSR effect on attachment. Whether one or both peptides modulate osteoblast differentiation was not known, nor was it known if they have the potential to modify cell response to RGD.

PLL-*g*-PEG waschoseninthisstudy becauseof its advantages in terms of its ease of functionalization, ease of synthesis, stability on titanium surfaces, and ability to resist protein adsorption (Tosatti 2003; Tosatti et al. 2003). PLL-*g*-PEG self-assembles on titanium as the positively charged PLL backbone adsorbs to the negatively charged titanium oxide surface layer, while the more hydrophilic PEG chains are presented at the surface. PLL-*g*-PEG has been shown to reduce protein adsorption to < 5 ng/cm^2 as well as to greatly reduce cell adhesion (Tosatti et al. 2003). The PEG chains can be functionalized at the terminal end, resulting in presentation of the biologically active ligand with minimal interference from adsorbed proteins or other sources (Tosatti et al. 2004). In the present study, rough titanium surfaces were coated with PLL-*g*-PEG with varying combinations of the peptides RGD and KRSR.

Methods

Surfaces

The substrates used were sand blasted, acid-etched surfaces (commercially known as SLA) on titanium disks supplied by Institut Straumann AG (Basel, Switzerland). The manufacture and characterization of SLA disks have been described extensively elsewhere (Tosatti 2003; Le Guehennec et al. 2007). The SLA surface has a complex morphology consisting of craters between 20 and 50 mm in diameter (from sandblasting) overlaid with micropits between 0.5 and 2 μm in diameter (from acid etching), such that the overall topography mimics that of osteoclast resorption pits (Boyan et al. 2003; Zinger et al. 2005). Roughness

values were estimated using laser noncontact profilometry to yield Ra and Rq values of 5.5 ± 0.3 and 6.91 ± 0.39 mm, respectively (Lossdorfer et al. 2004). specific surface area was measured with impedance spectroscopy to yield a value of 6.5 cm^2/cm^2 (Contu et al. 2003). This value is a measure of the effective SLA surface area divided by the geometrical area of a perfectly flat surface, indicating that SLA has an effective surface area 6.5 times that of a perfectly flat surface. The surface of the SLA naturally oxidizes to form a thin layer of titanium dioxide. Although SLA is hydrophobic with an advancing contact angle of 139.88° (Zhao et al. 2007; 2005; Rupp et al. 2006), the SLA substrates used in the present study were plasma cleaned before use and therefore, were hydrophilic.

Synthesis of PLL-*g*-PEG/PEG-peptide

Non-functionalized PLL-*g*-PEG was synthesized according to protocols by Huang et al. (2001) & Pasche et al. (2003). Poly(L-lysine) hydrobromide (PLL-HBr; Sigma-Aldrich, Buchs, CH, Switzerland) was dissolved in sodium borate buffer and sterilized with a 0.22 μm filter. Succinimide propionate methoxy-PEG (mPEG-SPA; Nektar Therapeutics, Bradford, UK) at a molecular ratio corresponding to a grafting ratio $g = 3.5$ was added and the reaction was allowed to proceed for 6 h at room temperature. Dialysis was performed first against phosphate-buffered saline (PBS, pH 7.4) and then deionized water each for 24 h before the product was freeze-dried and stored at −20°C.

PLL-*g*-PEG/PEG-peptide polymers were synthesized according to Schuler et al. (2006a). Peptides and *N*-hydroxysuccinimide polyethylene glycol vinylsulfone (NHS-PEG-VS, Nektar Therapeutics) were reacted for 5 min in a salt buffer solution containing 10 mM *N*-(2-hydroxyethyl)-piperazine-N′-2-ethanesulfonic acid (HEPES; Sigma-Aldrich) at pH 8.4. PLL hydro-bromide was dissolved in HEPES and added to the reaction. After 1 h, mPEG-SPA was dissolved in HEPES and added to the final mixture, which was stirred for 24 h at room temperature. Fifty microliters of β-mercaptoethanol (Fluka, Buchs, CH, Switzerland) was used for quenching. Before freeze-drying, the mixture was dialyzed against deionized water for 48 h. Deionized water was changed twice a day. Polymers resulted in a white powder and were kept frozen at −20°C before use. The peptide sequences used were *N*-acetyl-GCRGYG**RGD**SPG-NH_2, *N*-acetyl-GC RGYG**KRSR**G-NH_2, and *N*-acetyl-GCRGYG **KSSR**G-NH_2 (all purchased from JPT Peptide Technologies GmbH, Berlin, Germany). The Gly–Cys–Arg (GCR) sequence of the linker is critical because reaction occurs between the vinylsulfone group of PEG-VS and the thiol group of the cysteine. The Gly–Tyr–Gly (GYG) sequence is primarily used as a spacer, but is also used to measure grafting efficiency based on the specific hydrogen nuclear magnetic resonance (H-NMR) signal of the tyrosine. Neither peptide alone nor in sequence has been reported to have biological activity in osteoblasts.

As described previously, several quality control steps were taken to ensure appropriate synthesis and functionalization of each batch of polymer (Tosatti 2003; Tosatti et al. 2003). The grafting ratio *g* and degree of peptide functionalization were measured using H-NMR, and polymer adsorption was measured using optical waveguide lightmode spectroscopy (OWLS) (Pasche et al. 2003). The surface peptide densities were calculated as published elsewhere and are shown in Table 1 (Tosatti et al. 2003; Schuler et al. 2006a, 2006b).

Competitive binding was examined in earlierstudies andshowednopreferentialbinding between different PLL-*g*-PEG/PEG-peptide combinations (Tosatti et al. 2004). OWLS was also used to confirm resistance to protein adsorption of all PLL-*g*-PEG polymer surfaces in full serum, which was estimated at <5 ng/cm^2 (Tosatti et al. 2003).

Preparation of coated surfaces

Before coating SLA disks, frozen samples of PLL-*g*-PEG and peptide-functionalized PLL-*g*-PEG were warmed to room temperature, dissolved in a salt buffer solution (denoted hereafter as HEPES 2) containing 10 mM HEPES (MicroSelect, Fluka Chemie GmbH) and 150 mM NaCl at pH 7.4 (to reach a final concentration of 0.5 mg/ml), filter sterilized using a 0.22 mm filter (Milian, Basel, CH Switzerland), and used to prepare the designated peptide surface densities. Solutions containing PLL-*g*-PEG/PEG-peptide were mixed with non-functionalized PLL-*g*-PEG in order to yield desired surface peptide densities as described in Fig. 1b. Multi-peptide PLL-*g*-PEG surfaces were created by mixing solutions containing PLL-*g*-PEG/PEG-RGD and PLL-*g*-PEG/PEG-KRSR in varying peptide concentrations as shown in Fig. 1b. All SLA disks used in this study were sterilized using an oxygen plasma cleaner (PDC-32G, Harrick Plasma, Ithaca, NY, USA) for 5 min under low vacuum and then placed in 24-well plates. Solutions containing the desired polymer–peptide combinations were pipetted immediately onto the appropriate surfaces for 30 min followed by two washings in sterile HEPES 2 buffer solution.

Experimental design

Control groups included (1) TCPS, (2) plasma-cleaned titanium SLA, and (3) titanium SLA coated with unfunctionalized PLL-*g*-PEG. These groups are similar to the controls used in a previous study by Tosatti et al. (2004), which examined the dose-dependent effects of RGD functionalized to PLL-*g*-PEG. Experimental groups were formed by coating disks with PLLg-PEG solutions containing varying concentrations of RGD, KRSR (Fig. 1b), and KSSR. KRSR surface peptide density was varied from 0, 5, 10, 15, to 20 pmol/cm^2, and RGD surface peptide density was varied from 0, 0.05, to 1.26 pmol/cm^2. KSSR surface peptide density was 10 pmol/cm^2 in combination with RGD varied at surface peptide densities of 0, 0.05, and 1.26 pmol/cm^2.

Cell culture

MG63 osteoblast-like human osteosarcoma cells were obtained from the American Type Culture Collection (Rockville, MD, USA). This cell line has been used in numerous studies as a model to assess osteoblast responses to biomaterials (Boyan et al. 2001; Kartsogiannis & Ng 2004) and results have been positively correlated with osseointegration *in vivo* (Cochran et al. 1996; Buser et al. 2004). Cells were cultured on TCPS or 15-mm-diameter disks in 24-well plates (N = 6 independent cultures per variable) at an initial density of 10,000 cells/cm^2 as described previously (Wang et al. 2006).

Cell response

All groups were harvested 24 h after confluence was reached for the cells on TCPS. Media were collected and the cell layers were washed twice with DMEM. Cells were released from

the surfaces by two sequential 10 min incubations in 0.25% trypsin at 37°C to ensure that all cells were removed from the SLA surfaces. The cells were collected to measure cell number, total protein, and alkaline phosphatase specific activity while the media were used to measure osteocalcin, transforming growth factor beta-1 (TGFβ1), and prostaglandin E_2 (PGE_2) levels.

Cell number and total protein—Following trypsinization, cells were centrifuged and then resuspended in PBS. Cell number was determined using a Coulter automatic cell counter (Z1 cell and particle counter, Beckman Coulter, Fullerton, CA, USA). After counting, cells were centrifuged and then lysed using 0.05% Triton X-100 followed by three consecutive freeze-thaw cycles. The cell lysate was used to measure total protein levels and alkaline phosphatase activity. Total protein was measured using a commercially available kit (Micro/Macro BCA, Pierce Chemical Co., Rockford, IL, USA) and a fluorescence microplate reader.

Osteoblast differentiation markers—Alkaline phosphatase specific activity (orthophosphoric monoester phosphohydrolase, alkaline; E.C. 3.1.3.1) was assessed by measuring the release of *p*-nitrophenol from *p*-nitrophenylpho-sphate at pH 10.2 and normalizing activity to total protein. Osteocalcin was measured in the conditioned media using a commercially available radioimmunoassay kit (Human Osteocalcin RIA Kit, Biomedical Technologies, Stoughton, MA, USA). Osteocalcin levels were normalized to total cell number.

Autocrine and paracrine regulators—Measurement of active TGF-β1 was performed using an enzyme-linked immunoassay kit specific for human TGF-β1 (TGF-β1 $E_{max}^{\oplus}$ Immunoassay System, Promega Corp., Madison, WI, USA) before acidification of the conditioned media. Total TGF-β1 was measured by acidification of the media with HCl for 10 min at room temperature followed by neutralization with NaOH. The amount of latent TGF-β1 in the conditioned media was calculated by subtracting the amount of active TGF-b1 from the total TGF-β1. PGE_2 was measured using a commercially available competitive binding radioimmunoassay kit (PGE_2 RIA Kit, Perkin Elmer, Wellesley, MA, USA). Levels of TGF-β1 and PGE_2 were normalized to total cell number.

Statistical analysis

Each data point was calculated from six independent cultures (n=6) and is presented as the mean ± standard error of the mean (SEM). A power analysis showed that and N of six provided sufficient power to detect significant differences if present. The data were parametric. They were analyzed via analysis of variance (ANOVA) and significant differences between groups were determined using Bonferroni's modification of Student's *t*-test, with significance set at P <0.05. In addition, data for alkaline phosphatase activity and for osteocalcin production were also analyzed using Mann–Whitney tests. This statistical method identified the same significant differences that were identified using ANOVA and Bonferroni. All experiments were repeated to ensure the validity of the results. The data presented are from a representative experiment for each parameter. Observations were

consistent among experiments unless otherwise stated, although the absolute baselines value differed between experiments.

Results

Cell number was regulated by both surface roughness and surface chemistry. Cell number was lower on SLA surfaces compared with TCPS, and was lower on PLL-*g*-PEG surfaces than both SLA and TCPS (Fig. 2a). Functionalizing PLL-*g*-PEG with 1.26 pmol/cm^2 of RGD increased the cell number compared with PLL-*g*-PEG coated controls, restoring it to near-SLA levels (Fig. 2b). These results were expected and confirm earlier results by Tosatti et al. (2004). KSSR caused a further decrease in cell number compared with SLA and PEGylated surfaces. Cell number was partially restored on KSSR surfaces by the addition of RGD. The effects of KRSR were very weak. KRSR alone had no effect on cell number and only increased cell number at a relatively high peptide surface density of 15 pmol/cm^2 in combination with 1.26 pmol/cm^2 of RGD (Fig. 2b).

Alkaline phosphatase activity was also regulated by surface roughness and surface chemistry. Alkaline phosphatase activity was increased on SLA surfaces and was further increased on SLA surfaces coated with PLL-*g*-PEG (Fig. 3a). KSSR did not affect alkaline phosphatase specific activity. The addition of 0.05 or 1.26 pmol/cm^2 of RGD peptide decreased alkaline phosphatase activity (Fig. 3b). Addition of KRSR also caused a decrease in alkaline phosphatase activity, though not as strongly as the decrease caused by RGD. The effect of combining RGD and KRSR seemed to be dominated by RGD, because there was weak supplemental inhibition by KRSR even at high peptide densities.

Surface roughness and surface energy affected osteoblast differentiation as determined by osteocalcin levels. Osteocalcin levels increased on SLA surfaces and further increased on SLA surfaces coated with PLL-*g*-PEG (Fig. 4a). The addition of RGD at a concentration of 1.26 pmol/cm^2 significantly decreased levels of osteocalcin. KSSR further increased osteocalcin levels, but this effect was masked with the addition of RGD. KRSR alone did not affect osteocalcin levels (Fig. 4b). There was a slight decrease in osteocalcin levels on PLL-*g*-PEG/PEG-RGD(1.26)/ PEG-KRSR(15) surfaces, although no other pep-tide combinations showed any effect of KRSR.

Levels of autocrine and paracrine factors were also affected by changes in surface roughness and surface energy, and by the addition of bioactive peptides. Levels of latent and active TGF-b1 (Figs 5a and c) and PGE2 (Fig. 6a) were increased on SLA vs. TCPS, and were further increased on PLL-*g*-PEG-coated SLA surfaces. Addition of 1.26 pmol/cm^2 RGD to the PLL-*g*-PEG surfaces caused a significant decrease in levels of latent and total TGF-b1 (Figs 5b and d) and PGE2 (Fig. 6b), confirming earlier results (Tosatti et al. 2004). Levels of latent and active TGF-b1on KSSR-coated surfaces were not statistically different from PEGylated controls; however, KSSR did increase levels of PGE2 vs. PEGylated and SLA surfaces (Fig. 6a). Addition of 15 pmol/cm^2 of KRSR reduced levels of active and latent TGFb1 (Figs 5b and d) and the addition of 10, 15, or 20 pmol/cm^2 of KRSR reduced levels of PGE2 (Fig. 6b). Interaction effects between RGD and KRSR were not observed. RGD appeared to be the dominant cause of reduction in TGF-b1levels. Combining RGD and

KRSR caused further inhibition of PGE2 levels than using either ligand alone, but this combination did not lead to synergistic responses. Altogether, KRSR was observed to affect osteoblastic phenotype only at high surface peptide densities, and generally did not affect cell phenotype as strongly as RGD. Surprisingly, KSSR did promote an osteoblastic phenotype, shown by the decreased cell number and increased levels of osteocalcin and PGE_2.

Discussion

The results of this study support previous observations (Tosatti et al. 2004) showing that addition of attachment factors like RGD or KRSR to PEGylated surfaces promotes cell attachment and growth, but inhibits osteoblast differentiation. Addition of RGD to the PLL-*g*-PEG surface increased cell number but RGD addition also reduced markers for differentiation and local factor production. The effects of KRSR on cell number were weak compared with RGD; the peptide had no effect on cell number or osteocalcin levels, but it did cause a decrease in TGF-β1 and PGE_2 levels at high surface peptide densities. In combination, KRSR and RGD at high surface peptide densities caused a decrease in alkaline phosphatase activity, and levels of osteocalcin, TGF-β1, and PGE_2. Surprisingly, KSSR, which does not promote osteoblast attachment to TCPS (Dee et al. 1998), caused an increase in osteoblastic differentiation, and this effect was reduced by the addition of RGD. These results support the hypothesis that attachment and proliferation are differentially regulated and further support the hypothesis that osteoblast differentiation is favored by reduced cell spreading. The results also suggest that biomimetic surfaces can be engineered that optimize attachment and differentiation.

Previous studies had suggested that KRSR increased osteoblast attachment to TCPS (Dee et al. 1998). This observation was supported by reports by Schuler (2006); Schuler et al. (2006a, 2006b) using the non-fouling KRSR-functionalized PEG brush strategy described in the present study, in which KRSR influenced both attachment and migration of rat calvarial osteoblasts. Although KRSR increased outgrowth of osteoblasts from newborn rat calvarial bone chips after 8 days of incubation time, outgrowth on RGD-coated surfaces was much greater. Others have shown that human bone marrow stromal cells (hBMSCs) are sensitive to KRSR as well (Lee et al. 2007).

In the present study, we did not examine cell attachment per se but the number of cells remaining on the surface at time of harvest. Thus, we assessed the combined effects of attachment, proliferation, apoptosis, and anoikis. We found that KRSR did not increase cell number by itself, but did increase cell number in combination with RGD. This result confirms earlier observations that RGD supported greater proliferation of newborn rat calvarial cells than KRSR (Schuler 2006; Schuler et al. 2006a, 2006b). However, the previous report did indicate that KRSR increased cell number, while the current study does not. This difference may be due to the cell source or to differences in the state of maturation in the osteoblast lineage. The MG63 cell model we used is a relatively immature osteoblast cell line whereas the Schuler and colleagues group used primary newborn rat calvarial osteoblasts obtained as outgrowths from bone chips.

The functional role of KRSR may depend in part on its presentation to responding cells, which depends upon flanking amino acids, ligand pre-presentation, and spatial patterning. Previous studies showed that hBMSCs exhibited increased attachment and osteoblastic differentiation when cultured on surfaces functionalized with Y**KRSRYT** (Lee et al. 2007). This peptide has the same pattern of amino acids, X**BBXBX** (Cardin &-Weintraub 1989), as the KRSR peptide used in the present study (GCRGYG**KRSRG**), which supported attachment but not differentiation of MG63 cells. The differences in the two outcomes could arise from differences in cell source, or to differences in the flanking amino acids. In addition, the BMSCs were cultured on smoothused substrates, whereas we cultured cells on microstructured Ti substrates. The increased surface roughness may have altered the conformation of attached proteins and peptides. In addition, other components of the media such as lipids, sugars, and ions, adsorb to the surface and also affect protein conformation. In the present study, we used a PLL-g-PEG interlayer, making the presented peptide conformation more consistent than direct coating of the peptide on Ti. Moreover, the specific surface area of rough surfaces is different from smooth ones. It is possible that the increased surface area could lead tomore peptides presented to each cell. Thus, another possibility is that surface roughness altered cell response by increasing the number of ligands available for cell binding.

In contrast to KRSR, the KSSR peptide used in the present study did increase osteoblast differentiation. This result could arise from biological activity of the KSSR peptide itself. Alternatively, KSSR could promote differentiation by inhibiting cell attachment and spreading. It is proposed that seemingly subtle differences in peptide composition could account for significant differences in biological activity. Our results indicate that KRSR plays a weak inhibitory role on the differentiation of osteoblasts on PLL-*g*-PEG surfaces, though the KSSR results do support the possibility of strong biological activity for other ligands based on the X**BBXBX** design.

Osteoblast attachment is often one of the first properties of a peptide that researchers evaluate; however, this measure may not be a good indicator of whether a peptide will affect differentiation. As observed previously (Dee et al. 1998; Schuler et al. 2009), KRSR increased attachment, whereas KSSR did not. In contrast, KRSR did not increase osteoblast differentiation. Again as noted previously by Dee and colleagues, KSSR was not shown to affect osteoblast attachment, but our results indicate a potent effect on osteoblast differentiation. The additional information provided in the present study demonstrates that attachment and proliferation assessments alone are insufficient for characterizing the biological activity of peptides. Assays for differentiation should not be performed in follow-up studies, but should be used as a primary tool for characterizing the biological activity of peptides.

Successful multifunctional peptide surfaces should have the ability to increase the osteoblast population at the implant surface, increase osteoblastic differentiation of attached cells, and discourage the development of inflammation and fibrosis. However, the combinations of RGD and KRSR we used in this study did not achieve this goal with respect to *in vitro* demonstration of enhanced osteogenic differentiation of attached cells. The present study indicated that KSSR does stimulate expression of an osteogenic phenotype, and that this

effect was reduced rather than increased when used in combination with RGD. RGD has been used effectively in some clinical applications, although its bioactivity is still less than native fibronectin, which provides an important synergy site for the stimulatory effect of the RGD motif on osteoblast differentiation (Garcia & Reyes 2005; Morra 2006; Schuler et al. 2006a, 2006b). In the present study the peptides were presented randomly at the surface and not at defined distances/positions of cell-binding and heparin-binding sites as found in native tissues. Thus, it is possible that RGD and KRSR were not presented in an optimal orientation to enhance osteoblast differentiation. This is supported by previous studies demonstrating that proper spatial arrangement of heparin-and integrin-binding domains may enhance cell attachment and response, although these studies did not specifically consider KRSR (Dalton et al. 1995; Sharma et al. 1999).

Conclusion

The present study examined the effects of PLL-*g*-PEG-based multifunctional peptide surfaces on the enhancement of markers for osteoblast proliferation and differentiation. RGD was effective in increasing cell number on the PLL-*g*-PEG surface, but RGD inhibited differentiation present on the PLL-*g*-PEG surface. KRSR alone had no effect on cell number, but had a weak inhibitory effect on levels of osteoblast differentiation. KSSR promoted an osteogenic phenotype, shown by decreased cell number and increased levels of osteocalcin and PGE2. The combination of RGD with either KRSR or KSSR was dominated by the effects of RGD, although KRSR did further inhibit osteoblast differentiation and local factor production at high peptide densities and KSSR stimulated osteoblastic differentiation. The combination of RGD with KSSR or other osteogenic peptides functionalized to PLL-*g*-PEG could enhance osteointegration by promoting both initial osteoblast attachment and subsequent osteoblastic differentiation. This possibility will be explored in future studies. Multifunctional peptide surfaces offer the ability to gain control over the biological cues provided to cells at the surface. Choosing which combinations of biological cues is a daunting task, but one that will likely be necessary to achieve truly bioactive surfaces. It is important to note that the study described in this paper is *in vitro*. *In vivo* studies using multifunctional surfaces are needed to assess their clinical value.

Acknowledgements

The authors thank Michael Chervonski for his technical contributions and Dr. Marco Wieland for his advice and support. Institut Straumann AG (Basel, Switzerland) provided the Ti disks used in this study. The research was supported by a grant from the ITI Foundation for the Promotion of Oral Implantology (Basel, Switzerland; Project No. 326), the Swiss Federal Commission for Technology and Innovation CTI (Project No. 7404.2) the NSF (EEC 9731643) and NIH (AR052102).

References

Barber TA, Ho JE, De Ranieri A, Virdi AS, Sumner DR, Healy KE. Peri-implant bone formation and implant integration strength of peptide-modified p(aam-co-eg/aac) interpenetrating polymer network-coated titanium implants. Journal of Biomedical Materials Research A. 2007; 80:306–320.

Boyan BD, Lohmann CH, Dean DD, Sylvia VL, Cochran DL, Schwartz Z. Mechanisms involved in osteoblast response to implant surface morphology. Annual Review of Materials Research. 2001; 31:357–371.

Boyan BD, Schwartz Z, Lohmann CH, Sylvia VL, Cochran DL, Dean DD, Puzas JE. Pretreatment of bone with osteoclasts affects phenotypic expression of osteoblastlike cells. Journal of Orthopaedic Research. 2003; 21:638–647. [PubMed: 12798063]

Buser D, Broggini N, Wieland M, Schenk RK, Denzer AJ, Cochran DL, Hoffmann B, Lussi A, Steinemann SG. Enhanced bone apposition to a chemically modified sla titaniumsurface. Journal of Dental Research. 2004; 83:529–533. [PubMed: 15218041]

Cardin AD, Weintraub HJR. Molecular modeling of protein-glycosaminoglycan interactions. Arteriosclerosis. 1989; 9:21–32. [PubMed: 2463827]

Cavalcanti-Adam EA, Micoulet A, Blummel J, Auernheimer J, Kessler H, Spatz JP. Lateral spacing of integrin ligands influences cell spreading and focal adhesion assembly. European Journal of Cell Biology. 2006; 85:219–224. [PubMed: 16546564]

Cavalcanti-Adam EA, Volberg T, Micoulet A, Kessler H, Geiger B, Spatz JP. Cell spreading and focal adhesion dynamics are regulated by spacing of integrin ligands. Biophysical Journal. 2007; 92:2964–2974. [PubMed: 17277192]

Cochran DL, Nummikoski PV, Higginbottom FL, Hermann JS, Makins SR, Buser D. Evaluation of an endosseous titanium implant with a sandblasted and acid-etched surface in the canine mandible: radiographic results. Clinical Oral Implants Research. 1996; 7:240–252. [PubMed: 9151588]

Contu F, Elsener B, Bohni H. Characterization of implant materials in fetal bovine serum and sodium sulfate by electrochemical impedance spectroscopy. Ii. Coarsely sandblasted samples. Journal of BiomedicalMaterials Research A. 2003; 67:246–254.

Cutler SM, Garcia AJ. Engineering cell adhesive surfaces that direct integrin alpha5beta1 binding using a recombinant fragment of fibronectin. Biomaterials. 2003; 24:1759–1770. [PubMed: 12593958]

Dalton BA, McFarland CD, Underwood PA, Steele JG. Role of the heparin binding domain of fibronectin in attachment and spreading of human bone-derived cells. Journal of Cell Science. 1995; 108:2083–2092. Part 5. [PubMed: 7657726]

Dee KC, Andersen TT, Bizios R. Design and function of novel osteoblast-adhesive peptides for chemical modification of biomaterials. Journal of Biomedical Materials Research. 1998; 40:371–377. [PubMed: 9570067]

Dettin M, Conconi MT, Gambaretto R, Pasquato A, Folin M, Di Bello C, Parnigotto PP. Novel osteoblast-adhesive peptides for dental/orthopedic biomaterials. J Biomed Mater Res. 2002; 60:466–471. [PubMed: 11920671]

Elmengaard B, Bechtold JE, Soballe K. In vivo effects of rgd-coated titanium implants inserted in two bone-gap models. Journal of Biomedical Materials Research A. 2005; 75:249–255.

Garcia AJ. Get a grip: integrins in cell-biomaterial interactions. Biomaterials. 2005; 26:7525–7529. [PubMed: 16002137]

Garcia AJ, Reyes CD. Bio-adhesive surfaces to promote osteoblast differentiation and bone formation. Journal of Dental Research. 2005; 84:407–413. [PubMed: 15840774]

Germanier Y, Tosatti S, Broggini N, Textor M, Buser D. Enhanced bone apposition around biofunctionalized sandblasted and acid-etched titanium implant surfaces. A histomorphometric study in miniature pigs. Clinical Oral Implants Research. 2006; 17:251–257.

Healy KE, Rezania A, Stile RA. Designing biomaterials to direct biological responses. Annals of the New York Academy of Science. 1999; 875:24–35.

Huang NP, Michel R, Voros J, Textor M, Hofer R, Rossi A, Elbert DL, Hubbell JA, Spencer ND. Poly(l-lysine)-g-poly(ethylene glycol) layers on metal oxide surfaces: surface-analytical characterization and resistance to serum and fibrinogen adsorption. Langmuir. 2001; 17:489–498.

Kartsogiannis V, Ng KW. Cell lines and primary cell cultures in the study of bone cell biology. Molecular and Cellular Endocrinology. 2004; 228:79–102. [PubMed: 15541574]

Le Guehennec L, Soueidan A, Layrolle P, Amouriq Y. Surface treatments of titanium dental implants for rapid osseointegration. Dental Materials. 2007; 23:844–854. [PubMed: 16904738]

Lee JY, Choo JE, Choi YS, Lee KY, Min DS, Pi SH, Seol YJ, Lee SJ, Jo IH, Chung CP, Park YJ. Characterization of the surface immobilized synthetic heparin binding domain derived from human fibroblast growth factor-2 and its effect on osteoblast differentiation. Journal of Biomedical Materials Research A. 2007; 83:970–979.

Lossdörfer S, Schwartz Z, Wang I, Iohmann CH, Turner JD, Wieland M, Cochran DI, Boyan BD. Microrough implant surface topographies increase osteogenesis by reducing osteoclast formation and activity. Journal of Biomedical Material Research A. 2004; 70:361–369.

Morra M. Biochemicalmodification of titanium surfaces: peptides and ecm proteins. European Cells and Materials. 2006; 12:1–15. [PubMed: 16865661]

Pasche S, De Paul SM, Voros J, Spencer ND, Textor M. Poly(l-lysine)-graft-poly(ethylene glycol) assembled monolayers on niobium oxide surfaces: a quantitative study of the influence of polymer interfacial architecture on resistance to protein adsorption by tof-sims and in situ owls. Langmuir. 2003; 19:9216–9225.

Petrie TA, Capadona JR, Reyes CD, Garcia AJ. Integrin specificity and enhanced cellular activities associated with surfaces presenting a recombinant fibronectin fragment compared to rgd supports. Biomaterials. 2006; 27:5459–5470. [PubMed: 16846640]

Petrie TA, Raynor JE, Reyes CD, Burns KL, Collard DM, Garcia AJ. The effect of integrin-specific bioactive coatings on tissue healing and implant osseointegration. Biomaterials. 2008; 29:2849–2857. [PubMed: 18406458]

Pierschbacher MD, Ruoslahti E. Cell attachment activity of fibronectin can be duplicated by small synthetic fragments of the molecule. Nature. 1984; 309:30–33. [PubMed: 6325925]

Reyes CD, Garcia AJ. Alpha2beta1 integrin-specific collagen-mimetic surfaces supporting osteoblastic differentiation. Journal of Biomedical Materials Research A. 2004; 69:591–600.

Ruoslahti E. Rgd and other recognition sequences for integrins. Annual Review of Cell and Developmental Biology. 1996; 12:697–715.

Ruoslahti E, Pierschbacher MD. New perspectives in cell adhesion: rgd and integrins. Science. 1987; 238:491–497. [PubMed: 2821619]

Rupp F, Scheideler L, Olshanska N, de Wild M, Wieland M, Geis-Gerstorfer J. Enhancing surface free energy and hydrophilicity through chemical modification of microstructured titanium implant surfaces. Journal of Biomedical Materials Research A. 2006; 76:323–334.

Schuler M, Hamilton DW, Kunzler TP, Sprecher CM, de Wild M, Brunette DM, Textor M, Tosatti SG. Comparison of the response of cultured osteoblasts and osteoblasts outgrown from rat calvarial bone chips to nonfouling krsr and fhrrika-peptide modified rough titanium surfaces. Journal of Biomedical Materials and Research B Applied Biomaterials. 2009; 91:517–527.

Schuler M, Owen GR, Hamilton DW, de Wild M, Textor M, Brunette DM, Tosatti SG. Biomimetic modification of titanium dental implant model surfaces using the rgdsp-peptide sequence: a cell morphology study. Biomaterials. 2006a; 27:4003–4015. [PubMed: 16574219]

Schuler M, Trentin D, Textor M, Tosatti SG. Biomedical interfaces: titanium surface technology for implants and cell carriers. Nanomedicine. 2006b; 1:449–463. [PubMed: 17716147]

Schwartz Z, Raz P, Zhao G, Barak Y, Tauber M, Yao H, Boyan BD. Effect of micrometerscale roughness of the surface of ti6al4v pedicle screws in vitro and in vivo. The Journal of Bone and Joint Surgery America. 2008; 90:2485–2498.

Sharma A, Askari JA, Humphries MJ, Jones EY, Stuart DI. Crystal structure of a heparinand integrin-binding segment of human fibronectin. EMBO J. 1999; 18:1468–1479. [PubMed: 10075919]

Tosatti S. Functionalized titanium surfaces for biomedial applications: physico-chemical characterization and biological in vitro evaluation, Materials Engineering. 2003; 37 PhD thesis, Swiss Federal Institute of Technology (ETH Zurich), Zurich, Switzerland.

Tosatti S, De Paul SM, Askendal A, VandeVondele S, Hubbell JA, Tengvall P, Textor M. Peptide functionalized poly(l-lysine)-g-poly(ethylene glycol) on titanium: resistance to protein adsorption in full heparinized human blood plasma. Biomaterials. 2003; 24:4949–4958. [PubMed: 14559008]

Tosatti S, Schwartz Z, Campbell C, Cochran DL, VandeVondele S, Hubbell JA, Denzer A, Simpson J, Wieland M, Lohmann CH, Textor M, Boyan BD. Rgd-containing peptide gcrgygrgdspg reduces enhancement of osteoblast differentiation by poly(l-lysine)-graft-poly(ethylene glycol)-coated titanium surfaces. Journal of Biomedical Materials Research A. 2004; 68:458–472.

Wang L, Zhao G, Olivares-Navarrete R, Bell BF, Wieland M, Cochran DL, Schwartz Z, Boyan BD. Integrin beta1 silencing in osteoblasts alters substrate-dependent responses to 1,25-dihydroxy vitamin d3. Biomaterials. 2006; 27:3716–3725. [PubMed: 16569430]

Zhao G, Schwartz Z, Wieland M, Rupp F, Gels-Gerstorfer J, Cochran DI, Boyan BD. High surface energy enhances cell response to titanium substratemicrostructure. Journal of Biomedical Material Research A. 2005; 74:49–58.

Zinger O, Zhao G, Schwartz Z, Simpson J, Wieland M, Landolt D, Boyan B. Differential regulation of osteoblasts by substrate microstructural features. Biomaterials. 2005; 26:1837–1847. [PubMed: 15576158]

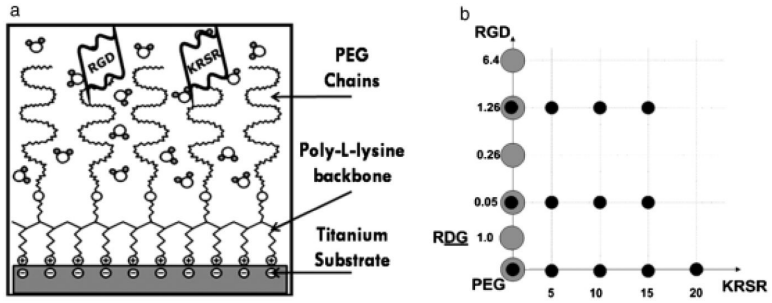

Fig. 1.

(a) Schematic of peptide-functionalized poly-L-Lysine grafted polyethylene glycol (PLL-*g*-PEG) following self-assembly on the titanium SLA surface. (b) Array showing the experimental groups used in this study to evaluate the interaction of RGD and KRSR. The large gray dots represent the previous study by Tosatti et al. (Tosatti et al. 2004) while the black dots represent groups used in the present study. Values are measured in pmol/cm^2. The dose-dependent response to RGD was measured with the following experimental groups coated on titanium SLA: (4) PLL-*g*-PEG/PEGRGD(0.05) and (5) PLL-*g*-PEG/PEG-RGD(1.26). The response to KSSR was measured with the following experimental groups coated on titanium SLA: (6) PLL-*g*-PEG/PEG-KSSR(10), (7) PLL-gPEG/PEG-RGD(0.05)/PEG-KSSR(10), and (8) PLL-*g*-PEG/PEG-RGD(1.26)/PEG-KSSR(10). The dose-dependent response to KRSR was measured with the following experimental groups coated on titanium SLA: (9) PLL-*g*-PEG/PEG-KRSR(5), (10) PLL-*g*-PEG/PEG-KRSR(10), (11) PLL-*g*-PEG/PEGKRSR(15), and (12) PLL-*g*-PEG/PEG-KRSR(20). Multifunctional peptide experimental groups included: (13) PLL-*g*-PEG/PEG-RGD(0.05)/PEGKRSR(5), (14) PLL-*g*-PEG/PEG-RGD(0.05)/PEGKRSR(10), (15) PLL-*g*-PEG/PEG-RGD(0.05)/PEGKRSR(15), (16) PLL-*g*-PEG/PEG-RGD(1.26)/PEGKRSR(5), (17) PLL-*g*-PEG/PEG-RGD(1.26)/PEGKRSR(10), and (18) PLL-*g*-PEG/PEG-RGD(1.26)/ PEG-KRSR(15). KRSR at a surface peptide density of 20 pmol/cm^2 was near the saturating surface peptide density and therefore could not be combined with RGD.

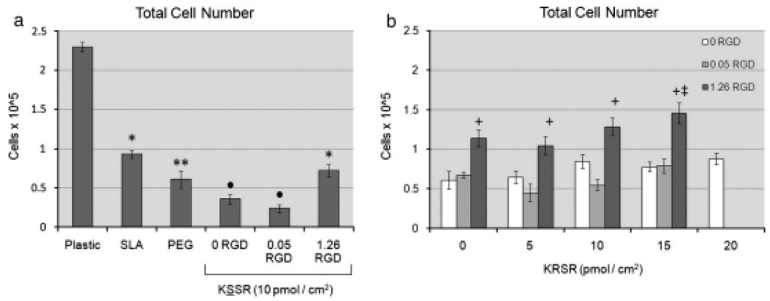

Fig. 2.

Effects of RGD, KRSR, and KSSR on cell number in osteoblast-like MG63 cells. (a) Cell number decreased on PLL-*g*-PEG surfaces compared with TCPS and SLA surfaces. Addition of KSSR further decreased cell number vs. PLL-*g*-PEG controls. (b) KRSR alone had no discernable effect on cell number. The combination of KRSR and RGO at a high peptide surface density increased cell number. (a) $^{*}P$ <0.05. Ti surfaces v. plastic; $^{**}P$<0.05, PEG surfaces vs. SLA; $^{\bullet}P$<0.05, KSSR vs. PEG. (b) +P<0.05. RGD vs. KRSR alone (0 RGO); ‡P<0.05, KRSR vs. RGD alone (0 KRSR).

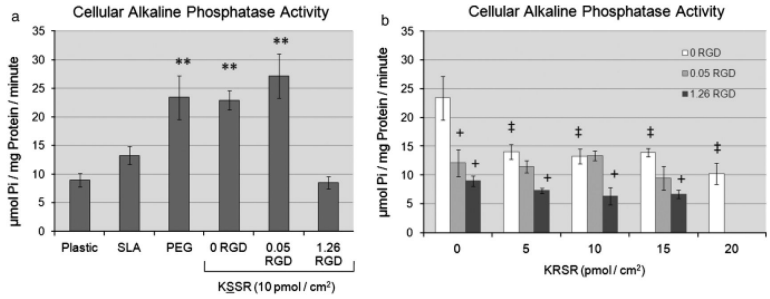

Fig. 3.

Effects of RGD, KRSR, and KSSR on alkaline phosphatase specific activity in osteoblast-like MG63 cells. (a) Alkaline phosphatase activity increased on PLL-*g*-PEG surfaces compared with TCPS and SLA surfaces . There was no effect of KSSR on alkaline phosphatase activity. (b) Addition of either RGD or KRSR decreased alkaline phosphatase activity. The effect of combining RGD and KRSR caused a further decrease in alkaline phosphatase activity at high peptide densities. (a) $^{**}P<0.05$, PEG surfaces vs. SLA. (b) $+P<0.05$, RGD vs. KRSR alone (0 RGD) ; ‡$P<0.05$, KRSR vs. RGD alone (0 KRSR).

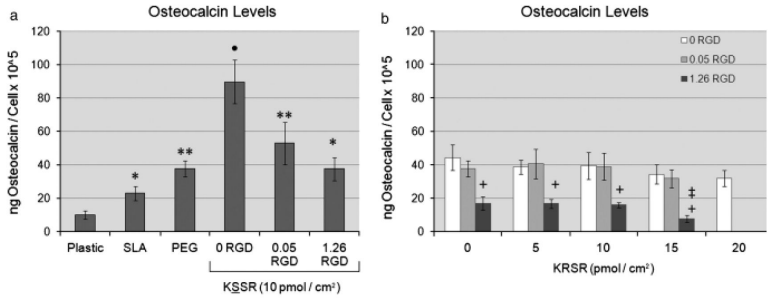

Fig. 4.

Effects of RGD, KRSR, and KSSR on osteocalcin levels in osteoblast-like MG63 cells. (a) Levels of osteocalcin increased on PLL-*g*-PEG surfaces compared with TCPS and SLA surfaces. The addition of 1.26 pmol/cm^2 RGD decreased levels of osteocalcin. Addition of KSSR increased osteocalcin levels. (b) KRSR alone did not affect osteocalcin levels, although the combination of RGD and KRSR at high peptide density decreased osteocalcin levels. (a) $^{*}P<0$ .05, Ti surfaces vs. plastic; $^{**}P<0.05$, PEG surfaces vs. SLA; $^{\bullet}P<0.$ 05. KSSR vs. PEG. (b) $+P<0.05$, RGD vs. KRSR alone (0 RGD) ; ‡$P<0.0$ 5, KRSR vs. RGD alone (0 KRSR) .

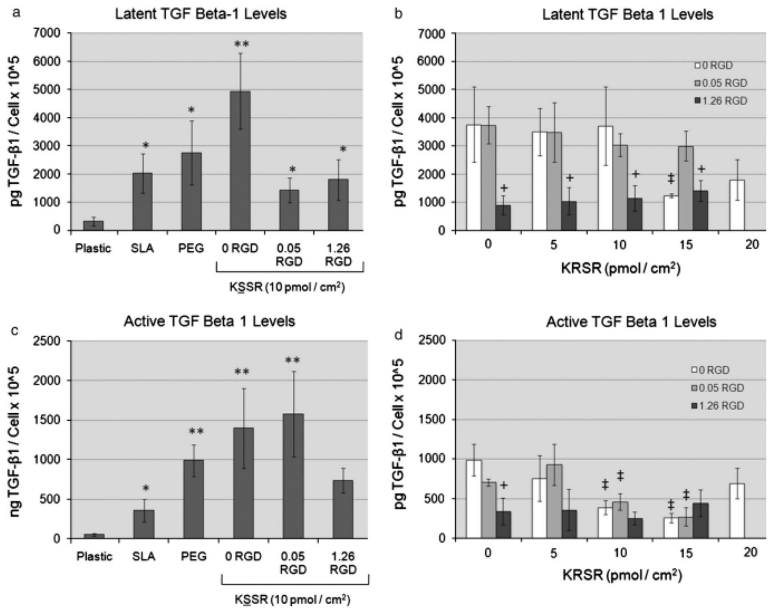

Fig. 5.

Effects of RGD, KRSR, and KSSR on TGF-b1 levels in osteoblast-likeMG63 cells. Levels of latent and active TGF-β1 were increased on PLL-g-PEG surfaces vs. TCPS and SLA surfaces (a,c). KSSR did not affect active or latent TGF-β1 levels. Addition of 1.26 pmol/cm^2 RGD reduced latent and active TGF-β1 levels, as did addition of 15 pmol/ cm^2 of KRSR (b,d). (a,c) $^{*}P<0.05$, Ti surfaces vs. plastic; $^{**}P<0.05$, PEG surfaces vs. SLA. (b,d) $+P<0.05$, RGD vs. KRSR alone (0 RGD); ‡$P<0.05$, KRSR vs. RGO alone (0 KRSR).

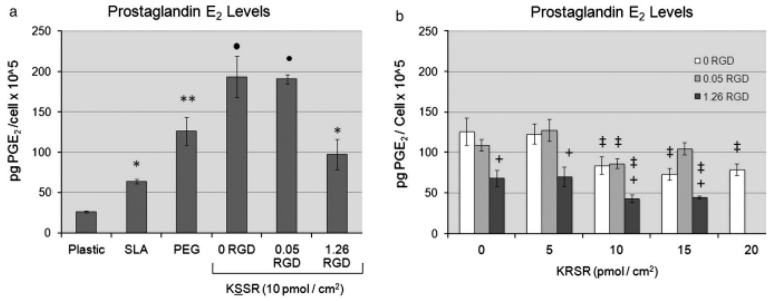

Fig. 6.

Effects of RGD, KRSR, and KSSR on PGE2 levels in osteoblast-like MG63 cells. (a) PGE2 levels were increased on PLL-g-PEG surfaces vs. TCPS and SLA surfaces. Addition of KSSR further increased levels of PGE2. (b) Addition of 1.26 pmol/cm^2 RGD reduced levels of PGE2, as did addition of KRSR. Combining RGD and KRSR caused further inhibition of PGE2, especially at high surface peptide densities. (a) *<*P*0.05, Ti surfaces vs. plastic;***P*<0.05, PEG surfaces vs. SLA. •*P*< 0.05, KSSR vs. PEG. (b) +*P*< 0.05, RGD vs. KRSR alone (0 RGD) ; ‡*P*<0.05, KRSR vs. RGD alone (0 KRSR).

Table 1

Molecular weight, grafting ratio, peptide functionalization, polymer/protein adsorption and peptide surface density for all polymers used in this study

	PEG	RGD	KRSR	KSSR
Molecular weight PLL (kDa)	15.9	15.9	15.9	15.9
Molecular weight lysine unit (kDa)	0.128	0.128	0.128	0.128
Molecular weight peptide (kDa)	–	1.222	1.197	1.128
Molecular weight entire polymer (kDa)	99.1	69.4	75	63.2
Grafting ratio, g [–] peptide-functionalized*	3.3	4	9.3	9.7
PEG-chains (%)*	–	8	76.3	50.1
Polymer adsorption (ng/cm^2)†	175	175	135	143
Protein adsorption (ng/cm^2)†	<5	<5	<5	<5
Peptide surface density, ρ_{ps} (pmol/cm^2)	–	5.1	20	15.8

*Measured with NMR technique.

†Measured with OWLS technique.